Quantum Interference in Radial Heterostructure Nanowires

Minkyung Jung,[†,⊗] Joon Sung Lee,[‡] Woon Song,[‡] Young Heon Kim,[‡] Sang Don Lee,[‡] Nam Kim,[‡] Jeunghee Park,[§] Mahn-Soo Choi,[⊥] Shingo Katsumoto,[∥] Hyoyoung Lee,[†,*] and Jinhee Kim[‡,*]

National Creative Research Initiative, Center for Smart Molecular Memory, Electronics and Telecommunication Research Institute, Daejeon 305-700, Korea, Korea Research Institute of Standards and Science, Daejeon 305-600, Korea, Department of Chemistry, Korea University, Jochiwon 339-700, Korea, Department of Physics, Korea University, Seoul 136-713, Korea, and Institute for Solid State Physics, University of Tokyo, Chiba 277-8581, Japan

ABSTRACT

Core/shell heterostructure nanowires are one of the most interesting mesoscopic systems potentially suitable for the study of quantum interference phenomena. Here, we report on experimental observations of both the Aharonov–Bohm (h/e) and the Altshuler–Aronov–Spivak ($h/2e$) oscillations in radial core/shell (In_2O_3/InO_x) heterostructure nanowires. For a long channel device with a length-to-width ratio of about 33, the magnetoresistance curves at low temperatures exhibited a crossover from low-field $h/2e$ oscillation to high-field h/e oscillation. The relationship between the oscillation period and the core width was investigated for freestanding or substrate-supported devices and indicated that the current flows dominantly through the core/shell interface.

The quantum mechanical nature of electron transport through mesoscopic conductors is manifested in various non-Ohmic transport properties such as conductance quantization,[1] universal conductance fluctuation,[2] and the violation of Kirchhoff's law,[3] all of which demonstrate strong differences from classical Ohmic transport. The prototype experiment demonstrating the importance of quantum mechanical phase coherence is the double slit experiment in which phase difference between the two paths of an electron result in an interference pattern. As demonstrated already in 1960s, when the two paths enclose an external magnetic flux Φ, the interference pattern is modulated periodically as a function of Φ with a period of $\Phi_0 = h/e$, where h is the Planck constant and e is the elementary charge.[4,5] If electrons pass through closed multiply connected conductors such as rings or cylinders (for the difference between the double-slit experiment and the closed-ring experiment, see ref 5), the interference among multiple loops around the enclosed flux

can, in principle, lead to the oscillation of the magnetoresistance (MR) with periods h/ne, where $n = 1, 2, 3$, and so on. In a true one-dimensional (1D) ring, where the wire is infinitely thin, the primary h/e oscillation completely dominates the others. For a ring with disordered wire of finite width, the visibility of the primary h/e oscillation gradually decreases and the secondary $h/2e$ oscillation becomes more prominent.[5] The crossover from h/e to $h/2e$ oscillation is tuned by the strength of the disorder and the width of the wire. Such crossover also happens in an array of rings due to the mesoscopic fluctuations, that is, the unavoidable fluctuation of ring size in the array. Cylindrical conductors are also expected to exhibit this crossover, since the effective ring size naturally fluctuates in the presence of disorder. The $h/2e$ oscillation is more robust against the disorder effects or the mesoscopic fluctuations because it originates from the interference between a pair of time-reversed paths, each of which forms a complete loop around the flux with the opposite sense of rotation; the fluctuations are in effect canceled. For this reason, the secondary $h/2e$ oscillations are commonly called the Altshuler–Aronov–Spivak (AAS) oscillations,[6] to be distinguished from primary h/e oscillation, known as the Aharonov–Bohm (AB) oscillation.[4]

Experimentally, the AB and/or AAS oscillations have been observed in a variety of systems. Both the AB and AAS oscillations have been reported in single metal[5] and semi-

---

* To whom correspondence should be addressed. E-mail: (J.K.) jinhee@kriss.re.kr; (H. L.) hyoyoung@etri.re.kr.
† National Creative Research Initiative, Center for Smart Molecular Memory, Electronics and Telecommunication Research Institute.
‡ Korea Research Institute of Standards and Science.
§ Department of Chemistry, Korea University.
⊥ Department of Physics, Korea University.
∥ University of Tokyo.
⊗ Present address: Korea Research Institute of Standards and Science, Daejeon 305-600, Korea.

conductor rings,[7−12] whereas the AAS oscillation alone has been observed in metal cylinders.[5,13] Several MR and magneto-optical measurements have reported the AB oscillations in carbon nanotubes,[14−17] and there is one MR experiment reporting the AAS oscillations.[18] Curiously, however, no experiment has observed both the AB and AAS oscillations in single carbon nanotube sample.

Here we report an experimental observation of both the AB and AAS oscillations in a new type of nanowire, the radial core/shell (In_2O_3/InO_x) heterostructure nanowire. Recently, several groups have successfully synthesized such core/shell heterostructure nanowires[19−24] and have achieved carrier mobility as high as 21 000 cm^2/Vs.[23,24] Despite such high mobility, until now neither the AB nor AAS oscillation has been observed in such nanowires.

Radial heterostructure nanowires, composed of a crystalline In_2O_3 core and an amorphous InO_x shell, were synthesized with the chemical vapor deposition method (Supporting Information). Initially, the crystalline In_2O_3 core was grown in an axial direction. The subsequent creation of the radial shell was achieved by altering the growth conditions in favor of homogeneous vapor-phase deposition of amorphous InO_x on the nanowire surface. In transmission electron microscope (TEM) studies, the thickness of the InO_x cover layer was found to fluctuate sample-to-sample from a few to over ten nanometers. Figure 1a shows a TEM image of a grown nanowire. The upper inset is a high-resolution TEM (HR-TEM) image of the core/shell interface; the lower inset is a selected-area electron diffraction (SAED) pattern in the crystalline In_2O_3 region. The HRTEM image, indicating that the nanowire grows along the [100] direction, shows a well-defined interface between the crystalline and the amorphous regions. The SAED pattern can be indexed along the [001] zone axis of In_2O_3 with cubic structure, which confirms that the nanowire grows along the [100] direction.

Our nanowires typically have the shape of a rectangular prism as shown in the scanning electron microscopy (SEM) image in Figure 1b.[25] The aspect ratios of the rectangular cross-sectional area were approximately 1−1.3; their overall widths were 20−150 nm. For the MR measurements, metallic electrodes were formed directly on the outermost surface of the nanowire (Figure 1b) such that the current could be injected into the shell of the nanowire. The right inset of Figure 1b shows a schematic view of the device. Details of the fabrication of nanowire devices are described elsewhere.[26]

We adopted a two-probe configuration for all MR measurements in this work (Supporting Information, Figure S1). The measured $I-V$ curves of our devices were almost linear down to a temperature of 40 mK. The resistance of the nanowires shows weak temperature dependence in the temperature range of 300 to 2 K; resistance was almost constant, especially at lower temperatures (Figure 2a). Typical resistance of the nanowires measured throughout this work was in the range of 10−50 kΩ at 2 K. To separately investigate the roles of the core and shell parts of the nanowires in the transport, we etched out the shell part of a nanowire by immersing the device in HCl solution for 60 s (insets, Figure 2b). Figure 2b shows $I-V$ curves before and
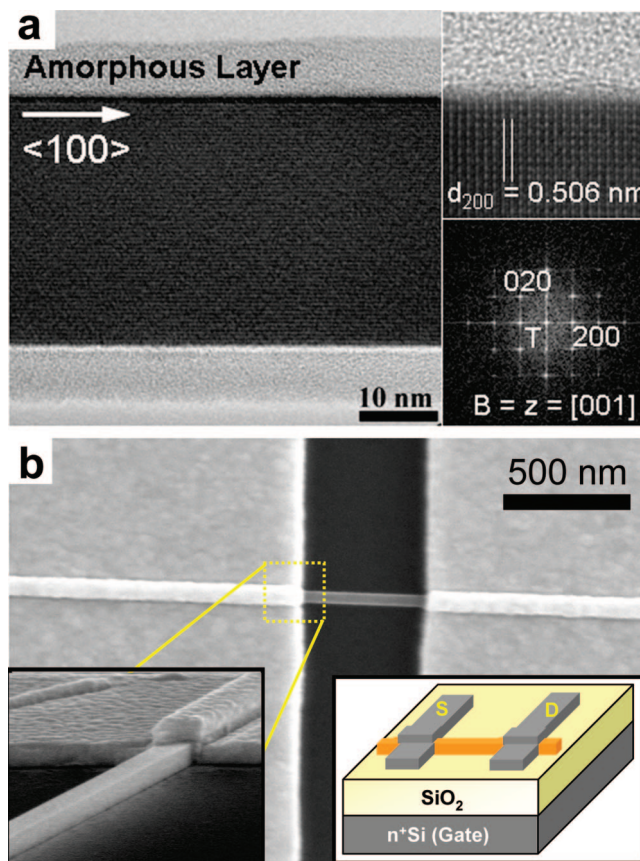
Figure 1. (a) Representative TEM images of the In_2O_3/InO_x core/shell heterostructure nanowires. Inset: HRTEM image of the core−shell nanowire (upper inset) and an SAED pattern in the crystalline In_2O_3 core region (lower inset). (b) SEM image of a nanowire device. Right inset is a schematic of the device.

after the etching process. With the shell etched out, the resistance increased by a factor of nearly 100 (from 0.04 to 3.3 MΩ) at 300 K. After the shell etching, there were no measurable AB or AAS oscillations in the resistance. From this, we concluded that the core part of the nanowire is highly resistive, indicating that the current flows dominantly through the shell or the core/shell interface.

We have measured MR of the nanowire devices at 2 K with the magnetic field applied parallel to the nanowire axes. In order to check the homogeneity of nanowire along the longitudinal direction, we fabricated two devices out of a single long nanowire. The length and width of the channel were 2.5 μm and 75 nm, respectively. We evaporated three electrodes onto the nanowire and measured MR of the upper (device A) and the lower (device B) parts separately. Inset of Figure 3a shows SEM image of devices A and B. The two devices exhibit almost identical MR features (Supporting Information, Figure S2), implying that each of our nanowires is quite uniform.

Figure 3a plots the measured MR (black curve) of device A. There are small oscillations superimposed on a large negative MR. With the smooth background subtracted, periodic oscillations are clearly seen as indicated by the red curve. The average peak-to-peak amplitude is larger than 300 Ω at low fields with a background of about 36 kΩ which corresponds to visibility, $\Delta R/R$ ($H = 0$), close to 1%. The
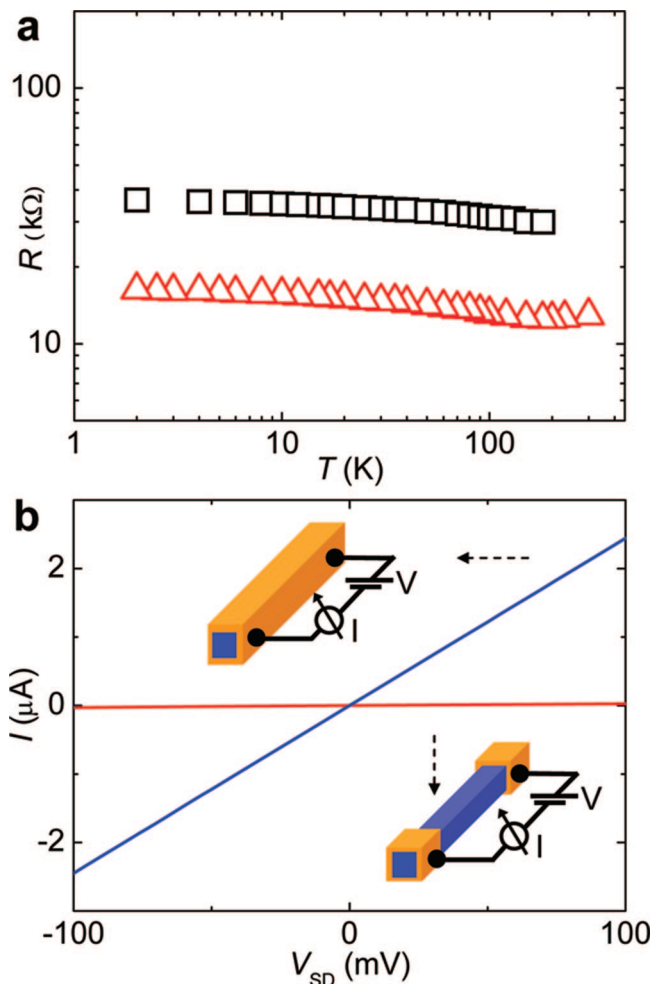
Figure 2. (a) Two-terminal resistance versus temperature of devices A ($W \approx 75$ nm, $L \approx 2.5$ μm) and D ($W \approx 80$ nm, $L \approx 500$ nm) correspond to rectangles and triangles, respectively. (b) $I–V$ characteristics obtained at room temperature before (blue) and after (red) etching the shell of nanowire. Insets: schematics of the devices before and after shell etching.

MR is almost symmetric about zero field, satisfying the Onsager relation, $R(H) = R(-H)$.[27] The oscillation period ΔH is 0.65 T at lower fields ($H < 2$ T) while $\Delta H = 1.3$ T at higher fields ($H > 2$ T). Taking 56×56 nm$^2 \approx 3200$ nm^2 for the dimensions of the flux-enclosing area, the period $\Delta H = 0.65$ T in field corresponds to the period $\Delta\Phi = h/2e$ in flux and $\Delta H = 1.3$ T to $\Delta\Phi = h/e$. The MR oscillations observed at low and high fields in the sample are thus identified as the AAS ($h/2e$) and AB (h/e) oscillations. We note that the value 56 nm of the lateral size of the flux enclosing area is substantially smaller than the overall width of the nanowire from the SEM measurement. As discussed below, this is consistent with the scenario in which the carriers reside mostly on the core/shell interface but not in the whole shell region. It is also noted that the period ΔH of the low-field oscillations has an angle dependence $\Delta H = 1/\cos\theta$, where θ is the tilt angle between the magnetic field and the nanowire axis (Supporting Information, Figure S3). Such behavior has also been reported in other systems.[8,14] As shown in Figure 3b, the MR was measured at various temperatures ranging from 2 to 10 K with steps of 2 K.
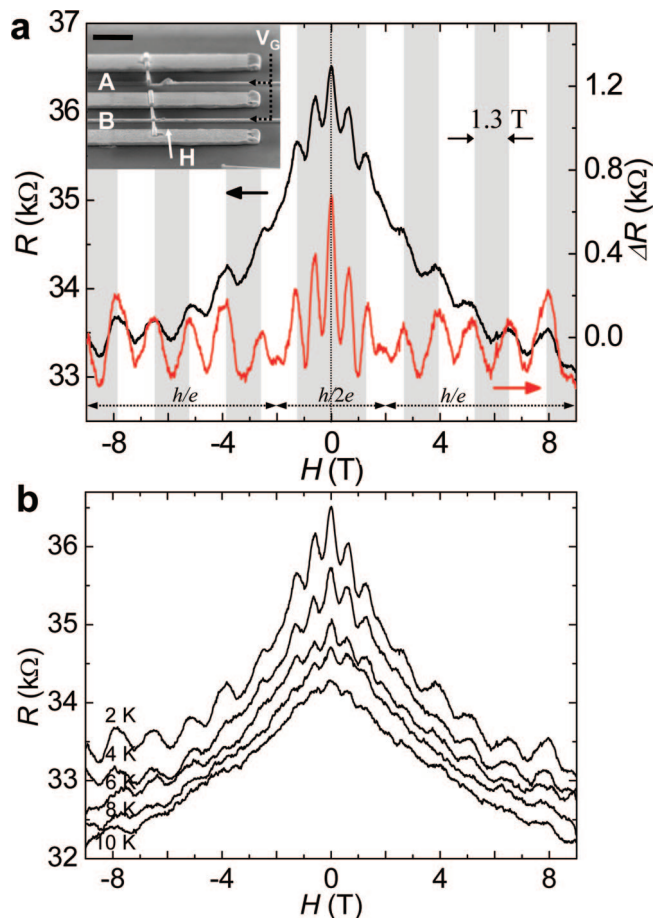
Figure 3. (a) The magnetoresistance (MR) curve of the device A measured at 2 K. The black curve (left scale) is the raw MR data; the red curve (right scale) is the same data with the background subtracted. The gray vertical stripes in the background indicate the h/e oscillation period ($\Delta H = 1.3$ T). The oscillatory part (red curve) of the MR data exhibits an AAS ($h/2e$) oscillation at lower field ($H < 2$ T) and an AB (h/e) oscillation at higher fields ($H > 2$ T). Inset: Tilted-view SEM image of the two devices (A and B) fabricated on a single nanowire. The length and width of the nanowires are 2.5 μm and 75 nm, respectively, for both devices. The scale bar is 500 nm. Narrow electrodes crossing the nanowire are top gate electrodes, insulated from the nanowire by a thin layer of aluminum oxide. Device A was broken accidentally during the subsequent measurements. (b) MR curves of device A at different temperatures.

Oscillations are observable up to 10 K, but are then smeared out with increasing temperature.

Ours is the first observation of AAS oscillation in heterostructure nanowires, although it has been reported before in metal cylinders.[5,13] Our observation of the AB oscillation with period h/e is even more remarkable since until now no experimental observation of this has been reported in metal or semiconductor cylinder systems, let alone in radial core/shell heterostructure nanowires. It has been suggested that AB oscillation with a flux period of h/e is supposed to be averaged out in long cylindrical samples.[5,13] According to the ensemble-averaging theory for a network of mesoscopic loops,[28] the amplitude of the oscillations will decrease proportionally to the square root of the number of loops, $N^{1/2}$. In the diffusive limit with many disorders, cylindrical shell (or hollow rectangular prism) conductors
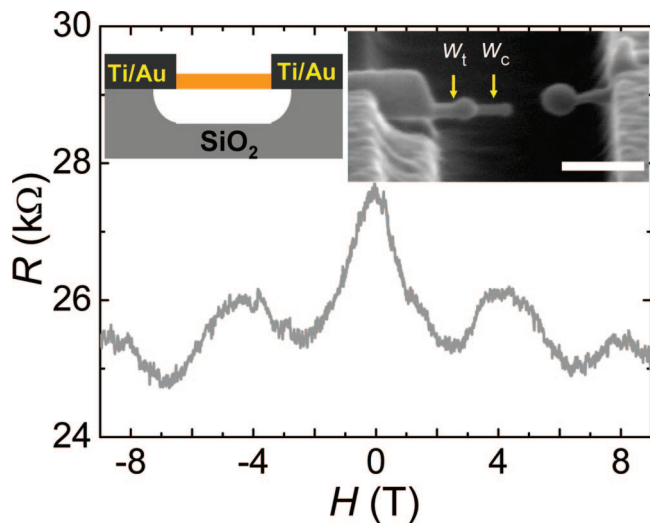
Figure 4. The MR curve of a suspended nanowire device C measured at 2 K. Left inset is a schematic of device structure. Right inset is an SEM image of the device taken after the breakdown caused by a high bias voltage. The width of the heterostructure nanowire (W_t) and the width of the core (W_c), marked by arrows, are ∼40 and 30 nm, respectively. The scale bar is 200 nm.

Table 1. Sample Dimensions and the Period ΔH of the AB oscillations[a]

sample	ΔH (T)	W_t (nm)	W_c* (nm)	$(W_t - W_c*)/2$ (nm)
A, B	1.3	76 (±3)	56	10
C	4.6	40 (±3)	30[b]	5
D	1.3	80 (±3)	56	12
E	1.7	65 (±3)	49	8
F	2	50 (±3)	45	3
G	3	41 (±3)	37	2

[a] W_t is the overall width of the nanowire measured by SEM. The effective width W_c* of the flux-enclosing area has been extracted from the relation $\Delta H = \Phi_0/(W_c*)^2$. [b] On sample C with suspended nanowire, the width W_c of the core part was also directly measured by SEM after burning out the shell part; this width value was identical to the value $W_c* = 30$ nm extracted from ΔH.

may be regarded as roughly equivalent to numerous ring-shaped conductors connected in series; as such, one can expect only AAS oscillation, as confirmed by the theory.[5,13] In the opposite limit, namely, in the ballistic limit without disorders, one can expect the AB oscillation, based on the modulation of density of states due to the external magnetic flux.[7,12,29,30] Our sample is considered to be in the intermediate regime between the diffusive and the ballistic limits. To our knowledge, there is no theory for the MR of cylindrical conductors in this quasi-ballistic regime.

The remaining question is "Where do the carriers reside?" Above, we have mentioned that the core part does not contribute to transport. Is transport then wholly through the shell part or along the core/shell interface? To address this question and test the influence of the substrate, we prepared a device (device C) with suspended nanowire, as shown in the inset of Figure 4, and performed electrical breaking experiment. It was found that this device is not subject to the influence of the substrate. Before breaking the nanowire, we measured its MR (Figure 4). The AB oscillation in the MR had a period of 4.6 T, which corresponded to a core width of 30 nm. As the bias voltage was increased, the nanowire broke near its midpoint due to Joule heating (Supporting Information, Figure S4). The right inset of Figure 4 shows an SEM image of the broken device, in which the core part of the nanowire is exposed by the melting of the shell part. The measured width of the core, $W_c \sim 30$ nm, is identical to the value estimated from the AB oscillation period and is substantially smaller than the overall width 40 nm. This observation suggests that the carriers may reside on the core/shell interface rather than wholly in the shell region. This was also the case for all six devices reported in this work. Table 1 lists the sample dimensions and the AB oscillation period of our sample. The effective width W_c* of the flux enclosing area extracted from the AB oscillation period ΔH are substantially smaller than the overall width

W_t of the nanowires. These values of W_c* are also consistent with the observations from our TEM measurements of other nanowires from the same batch, according to which the shell thickness range is 2−10 nm. It also suggests that transport in our heterostructure nanowires may occurs through the core/shell interface. The MR measurement was also made for device D, which exhibited h/e oscillations with period of $\Delta H \approx 1.3$ T (Supporting Information, Figure S5).

It is also worth noting that the visibility of the AB oscillation for device C is 1−5%, which is about 10−100 times larger than those of metallic rings or cylinders[5] and comparable to the results of two-dimensional electron gas systems (2DEGs).[9−12] Furthermore, the AB oscillations from our devices are robust enough to be observed in high magnetic fields; their amplitudes even tend to increase with increasing magnetic fields in some devices. These results suggest that there is a well-defined cross section area enclosed by the conducting electrons in each of the nanowires. Otherwise, the AB oscillation would diminish with the increase of the magnetic field. This is also consistent with the hypothesis that the main contribution to transport comes from the core/shell interface. In short, although we have no direct evidence of the formation of a 2DEG-like interface state in our nanowires, experimental data suggest that the dominant current flow may occur through the interface between the core and the shell.

In conclusion, we have observed quantum interference effects in the MR of core/shell (In_2O_3/InO_x) heterostructure nanowires grown by chemical vapor deposition into a rectangular prism shape. Both AB and AAS oscillations were identified in the MR curve of single nanowires. The visibility of the AB oscillation of the nanowire was 10−100 times greater than that of a metal ring and was comparable to that of a 2DEG ring and carbon nanotube. The relationship between the oscillation period and the core width was investigated for several nanowire devices in freestanding or substrate-supported state, which indicated that the current flows dominantly through the core/shell interface. Our observation clearly demonstrates the potential application of heterostructure nanowires as phase coherent quantum transport devices.

Supporting Information Available: Synthesis of hetero-structure nanowire. Four- and two-probe measurements (Figure S1). Magnetoresistance (MR) for device A and B (Figure S2). Angle-dependence of the $h/2e$ oscillation (Figure S3). Current−voltage ($I−V$) curve measured at high voltage for device C (Figure S4). Resistance versus magnetic field for device D (Figure S5). This material is available free of charge via the Internet at http://pubs.acs.org.

References

(1) van Wees, B. J.; van Houten, H.; Beenakker, C. W. J.; Williamson, J. G.; Kouwenhoven, L. P.; van der Marl, D.; Foxon, C. T. *Phys. Rev. Lett.* **1988**, *60*, 848.
(2) Lee, P. A.; Stone, A. D.; Fukuyama, H. *Phys. Rev. B* **1987**, *35*, 1039.
(3) Gabelli, J.; Feve, G.; Berroir, J.-M.; Placais, B.; Cavanna, A.; Etienne, B.; Jin, Y.; Glattli, D. C. *Science* **2006**, *313*, 499.
(4) Aharonov, Y.; Bohm, D. *Phys. Rev.* **1959**, *115*, 485.
(5) Aronov, A. G.; Sharvin, Y. V. *Rev. Mod. Phys.* **1987**, *59*, 755.
(6) Altshuler, B. L.; Aronov., A. G.; Spivak, B. Z. *Pisma Zh. Eksp. Teor. Fiz.* **1981**, *33*, 101.
(7) Lorke, A.; Luyken, R. J.; Govorov, A. O.; Kotthaus, J. P.; Garcia, J. M.; Petroff, P. M. *Phys. Rev. Lett.* **2000**, *84*, 2223.
(8) Bayer, M.; Korkusinski, M.; Hawrylak, P.; Gutbrod, T.; Michel, M.; Forchel, A. *Phys. Rev. Lett.* **2003**, *90*, 186801.
(9) Datta, D.; Melloch, M. R.; Bandyopadhyay, S.; Noren, R. *Phys. Rev. Lett.* **1985**, *55*, 2344.
(10) Timp, G.; Chang, A. M.; Cunningham, J. E.; Chang, T. Y.; Mankiewich, R.; Behringer, R.; Howard, R. E. *Phys. Rev. Lett.* **1987**, *58*, 2814.
(11) Yacoby, A.; Heiblum, M.; Mahalu, D.; Shtrikman, H. *Phys. Rev. Lett.* **1995**, *74*, 4047.
(12) Fuhrer, A.; Luscher, S.; Ihn, T.; Heinzel, T.; Ensslin, K.; Wegscheider, W.; Bichler, M. *Nature* **2001**, *413*, 822.
(13) Sharvin, D. Y.; Sharvin, Y. V. *Pisma Zh. Eksp. Teor. Fiz.* **1981**, *34*, 285.
(14) Fujiwara, A.; Tomiyama, K.; Suematsu, H.; Yumura, M.; Uchida, K. *Phys. Rev. B* **1999**, *60*, 13492.
(15) Zaric, S.; Ostojic, G. N.; Kono, J.; Shaver, J.; Moore, V. C.; Strano, M. S.; Hauge, R. H.; Smalley, R. E.; Wei, X. *Science* **2004**, *304*, 1129.
(16) Coskun, U. C.; Wei, T.-C.; Vishveshwara, S.; Goldbart, P. M.; Bezryadin, A. *Science* **2004**, *304*, 1132.
(17) Lee, J.-O.; Kim, J.-R.; Kim, J.-J.; Kim, J.; Kim, N.; Park, J. W.; Yoo, K.-H.; Park, K.-H. *Phys. Rev. B* **1999**, *61*, 16362.
(18) Bachtold, A.; Strunk, C.; Salvetat, J.-P.; Bonard, J.-M.; Forro, L.; Nussbaumer, T.; Schonenberger, C. *Nature* **1999**, *397*, 673.
(19) Lauhon, L. J.; Gudikson, M. S.; Wang, D.; Lieber, C. M. *Nature* **2002**, *420*, 57.
(20) Lu, W.; Xiang, J.; Timko, B. P.; Wu, Y.; Lieber, C. M. *Proc. Natl. Acad. Sci. U.S.A.* **2005**, *102*, 10046.
(21) Skold, N.; Karlsson, L. S.; Larsson, M. W.; Pistol, M.-E.; Seifert, W.; Tragardh, J.; Samuelson, L. *Nano Lett.* **2005**, *5*, 1943.
(22) Xiang, J.; Lu, W.; Hu, Y. J.; Wu, Y.; Yan, H.; Lieber, C. M. *Nature* **2006**, *441*, 489.
(23) Li, Y.; Xiang, J.; Qian, F.; Gradecak, S.; Wu, Y.; Yan, H.; Blom, D. A.; Lieber, C. M. *Nano Lett.* **2006**, *6*, 1468.
(24) Jiang, X.; Xiong, Q; Nam, S.; Qian, F.; Li, Y.; Lieber, C. M. *Nano Lett.* **2007**, *7*, 3214.
(25) Liang, C.; Meng, G.; Lei, Y.; Phillipp, F.; Zhang, L. *Adv. Mater.* **2001**, *13*, 1330.
(26) Jung, M.; Lee, H.; Moon, S.; Song, W.; Kim, N.; Kim, J.; Jo, G.; Lee, T. *Nanotechnology* **2007**, *18*, 435403.
(27) Buttiker, M. *Phys. Rev. Lett.* **1986**, *57*, 1761.
(28) Umbach, C. P.; Haesendonck, C. V.; Laibowitz, R. B.; Washburn, S.; Webb, R. A. *Phys. Rev. Lett.* **1986**, *56*, 386.
(29) Chakraborty, T.; Pietilainen, P. *Phys. Rev. B* **1994**, *50*, 8460.
(30) Iye, Y.; Ueki, M.; Endo, A.; Katsumoto, S. *Supperlattices Microstruct* **2003**, *34*, 165.

NL801506W